Supporting Information

Promoting Nanoparticle Delivery Efficiency to Tumor by Locally Increasing Blood Flow there

Feng Fan[1,2,3], *Bin Xie** [1], *and Lihua Yang** [1,2,3]

[1] Hefei National Laboratory for Physical Sciences at the Microscale, [2] CAS Key Laboratory of Soft Matter Chemistry, [3] School of Chemistry and Materials Science, University of Science and Technology of China, Hefei, Anhui 230026 China

Corresponding Author

(L.Y.) *E-mail: lhyang@ustc.edu.cn

(B.X.) *E-mail: bxie@ustc.edu.cn

ADDITIONAL TABLES AND FIGURES

Table S1. Anticancer nanomedicines approved for use in clinics.[1, 2]

Name	Drug	Nanocarriers	Indications	Approved country	Year
Genexol®-PM	Paclitaxel	Micelle	Breast, lung, pancreatic cancer, Recurrent breast cancer	Korea	2007
Abraxane®	paclitaxel	Albumin	Metastatic breast cancer	USA	2005
Doxil/Caelix®	Doxorubicin	Liposome	Ovaria, metastatic breast cancer, Kaposi sarcoma	USA	1995
Myocet®	Doxorubicin	Liposome	Breast cancer	EU	2000
DaunoXome®	Daunorubicin	Liposome	Kaposi Sarcoma	USA	1996
Depocyt®	Cytabirine	Liposome	Lymphomatus meningitis	USA/EU	1999
Marqibo®	Vincristine	Liposome	Leukemia	USA	2012
Mepact®	Osteosarcoma	Liposome	Mifamurtide	EU	2009
Onivyde® (MM-398)	Irinotecan	Liposome	Metastatic pancreas cancer	USA	2015
Lipusu®	Paclitaxel	Liposome	NSCLC, breast cancer	China	2015
PICN®	Paclitaxel	Liposome	Metastatic breast cancer	India	2014
Vyxeos® (CPX-351)	Cytarabine and daunorubicin (5:1)	Liposome	High-risk acute myeloid leukemia	USA	2017

Table S2. Summary of Tumor Delivery Efficiency [3].

estimated on the basis of PBPK model				AUC Method
DE_{Tlast}	DE_{24}	DE_{168}	DE_{max}	DE_{Tlast_PK}
0.76	0.76	0.35	1.00	0.71

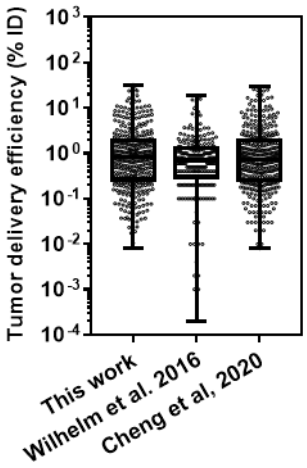

Figure S1. Analyses on nanoparticles delivery efficiencies using non-physiologically based pharmacokinetic modeling (Wilhelm et al. 2016 and this work) or physiologically based pharmacokinetic modeling (Cheng et al. 2020). The boxes represent the 25th to 75th percentiles, and the solid lines in the boxes indicate the median values. The error bar indicates the data value from minimum to maximum.

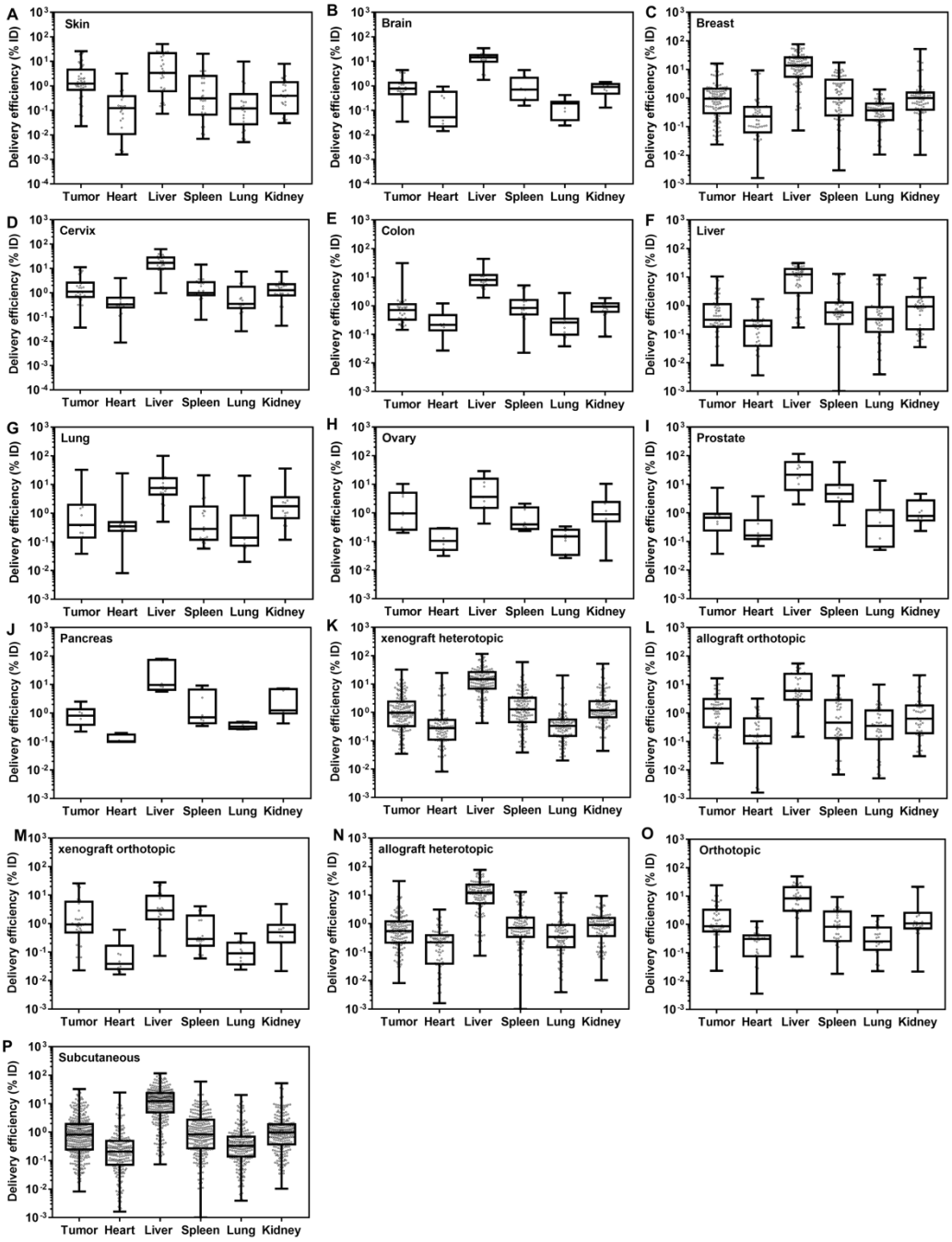

Figure S2. Subgroup analyses on nanoparticles delivery efficiencies estimated at tumor and the five organs (which are heart, liver, spleen, lung, kidney) using biodistribution profiles on anti-tumor nanoparticles in the dataset[3]. (A-J) Cancer types include (A) Skin, (B) Brain, (C) Breast, (D) Cervix, (E) Colon, (F) Liver, (G) Lung, (H) Ovary, (I) Prostate, and (J) Pancreas. (K-P) Tumor models are (K) xenograft heterotopic, (L)

allograft orthotopic, (M) xenograft orthotopic, (N) allograft heterotopic, (O) orthotopic, and (P) subcutaneous. The boxes represent the 25th to 75th percentiles, the solid lines in the boxes indicate the median values, and the error bars incidate the data value from minimum to maximum.

Table S3. The median or mean value of nanoparticle delivery efficiency in each organ/tumor according to meta-analysis.

	Tumor (n=382)	Heart (n=227)	Liver (n=327)	Spleen (n=292)	Lung (n=252)	Kidney (n=283)
Median (%ID)	0.83	0.22	11.58	0.83	0.32	0.96
Mean ± S.D. (%ID)	2.27±4.23	0.67±2.03	16.51±17.47	2.54±5.15	0.93±2.18	2.39±5.47

Table S4. The numbers of total cells and resident macrophages in liver, spleen, and kidney.

Tissue	Weight(g)	Total cells ($\times 10^6$ cell/g)	Macrophages ($\times 10^6$ cell)	Ref
Liver	1.5	~23	~6.1	4
Spleen	0.164	~1500	~3.99	5
Kidney	~0.3	NA	~0.3	6
Lung	~0.1-0.2g	NA	~0.4	7

Table S5. Typically reported weights for major organs of Balb/C mice in the literature[8].

Organs	Heart	Liver	Spleen	Lung	Kidney
Weight(g)	0.133	1.013	0.106	0.130	0.274

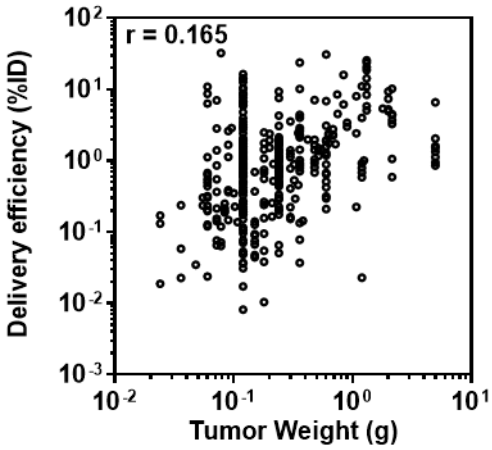

Figure S3. Correlation plots for tumor weight and nanoparticle delivery efficiency in tumor.

Table S6. The nanoparticle delivery efficiency for tumor subgroups with different weights.

Tumor Weight (g)	0-0.2 (n=211)	0.2-0.4 (n=87)	0.4-0.6 (n=30)	0.6-0.8 (n=9)	0.8-1.0 (n=4)	>1.0 (n=41)
Median (%ID)	0.47	0.86	1.33	2.33	4.80	3.99
Mean ± S.D. (%ID)	1.66±3.48	1.63±2.99	2.59±5.58	3.18±2.16	7.16±6.09	5.86±6.55

Table S7. The blood flow rate of each organ of 20~30g mice reported in the literature.

	Liver	Spleen	Lung	Kidney	Ref
Blood Flow (mL/h)	132.9	18.85	4.713	85.77	[9]
	108	5.4	2.4	78	[10]
	56.7	2.76	15	25.1	[11]
	108	5.4		78	[12]
	127.82	5.78	2.73	80.24	[13]
Mean Blood Flow (mL/h)	106.7±30.15	7.64±6.38	6.21±5.95	69.42±24.98	

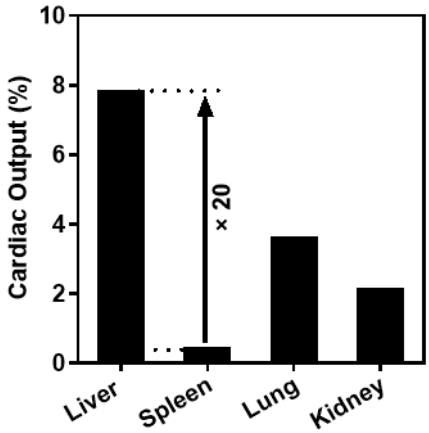

Figure S4. The cardiac output of each organ of 20~30g Balb/C mice reported in the literature[11].

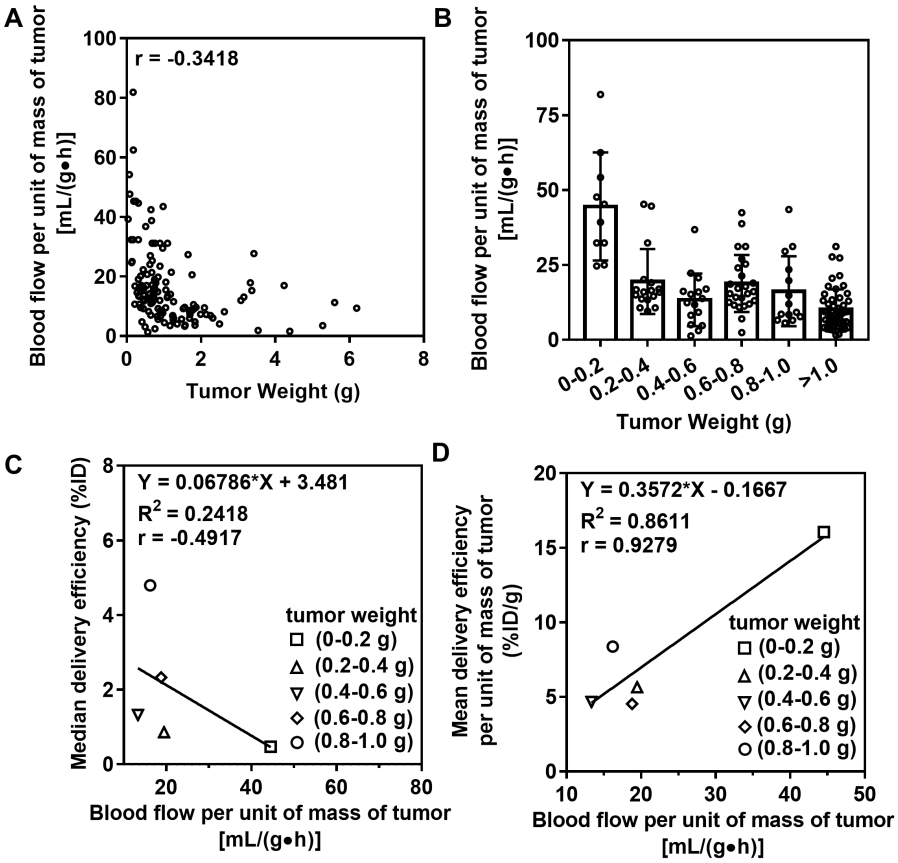

Figure S5. (A) Correlation plots for tumor weight and blood flow per unit of mass of tumor[14, 15]. (B) The blood flow per unit of mass of tumor between different tumor mass intervals according to (A). (C) The relationship of tumor-targeted nanoparticles' median delivery efficiency *versus* tumor blood flow per unit of mass of tumor (mean value). (D) The relationship of tumor-targeted nanoparticles' mean delivery efficiency per unit of mass of tumor *versus* tumor blood flow per unit of mass of tumor (mean value). Bars are reported as mean ± standard deviation. The correlation between metrics was estimated using Pearson correlation coefficients (r). For each comparison, r was determined with all datasets Correlation coefficients between metrics were interpreted as follows: $|r| < 0.3$, no relationship; $0.3 < |r| < 0.5$, weak relationship; $0.5 < |r| < 0.7$, moderate relationship; $|r| > 0.7$, strong relationship[16].

Table S8. The tumor blood flow before and after local mild hyperthermia.

Tumor	Processing method	Tumor weight (g)	Tumor blood flow mL/ (100 g• min) (before heat)	Tumor blood flow mL/ (100 g• min) (after heat)	Ref
R33230 AC	preheating at 42 ºC for 60 min, waiting for 24 h, and then heating at 42.5 ºC for 90 min	0.44	23.9 ± 1.8	61.0 ± 4.4	17
Mammary adenocarcinoma 13762A.	heating at 43.5 ºC for 1 h	0.03-0.2	14.08 ± 3.49	31.55± 6.00	18
		0.2-0.5	9.51 ± 1.37	11.97± 2.71	
		0.5-1.0	6.48 ± 0.68	17.14± 3.04	
		1.0-2.2	5.17 ± 0.94	9.54 ± 1.20	
R3230 AC	heating at 41.5 ºC for 30 min	0.8	~30.92	40.05 (end of heating) 62.91 (24-h later)	19
	heating at 40.5 ºC for 60 min		~30.53	38.96 (end of heating) 68.61 (24-h later)	

Table S9. Summary of tumor types whether local mild hyperthermia could increase tumor blood flow.

Increase tumor blood flow	without Increase tumor blood flow
MDA-MB-231 tumors[20]	4T1 tumor[20]
LS180 tumor[21, 22]	SMT-2A[23]
D-54 MG tumors[24-26]	Walker-256 Carcinoma[27]
human colon HT-29 tumor[28]	SCK tumor[15]
human head and neck carcinoma (FaDu cell)[29]	
R33230 AC[17, 19]	
Mammary adenocarcinoma 13762A[18].	
CT26 tumors[30]	

Table S10. Summary on strategies reported to be able to promote tumor blood perfusion.

Therapeutic agents	Target	Tumor Model	Vessel diameter/density	Tumor blood perfusion	Ref
ridegib	Stromal cells	Pancreatic ductal carcinoma	↑	↑	31, 32
EGPH20	Hyaluronan	Pancreatic ductal carcinoma	↑	↑	33, 34
1D11	Collagen	Mammary carcinoma	↑	↑	35
Losartan	Stromal cells, hyaluronan, collagen	Pancreatic ductal carcinoma	↑	↑	36
BQ123	ETA receptor	human U87 MG glioblastomas	Not reported	↑	37
cilengitide	endothelial cells	pancreatic cancer	↑	↑	38
Trastuzumab	vessel	HER2+ breast cancer	↑	↑	39
TNFa-CSG	ECM	Breasst cancer	Not reported	↑	40
Immune checkpoint blockade	CD8+ T cell	Breast/colon cancer	↓	↑	41
thalidomide	vessel	Breast/colon cancer	↑	↑	42

REFERENCES

1. Danhier, F., To exploit the tumor microenvironment: Since the EPR effect fails in the clinic, what is the future of nanomedicine? *J. Controlled Release* **2016,** *244*, 108-121.
2. Ragelle, H.; Danhier, F.; Préat, V.; Langer, R.; Anderson, D. G., Nanoparticle-based drug delivery systems: a commercial and regulatory outlook as the field matures. *Expert Opin. Drug Delivery* **2017,** *14* (7), 851-864.
3. Cheng, Y.-H.; He, C.; Riviere, J. E.; Monteiro-Riviere, N. A.; Lin, Z., Meta-analysis of nanoparticle delivery to tumors using a physiologically based pharmacokinetic modeling and simulation approach. *ACS Nano* **2020,** *14* (3), 3075-3095.
4. Crofton, R.; Diesselhoff-den Dulk, M. M.; Furth, R. v., The origin, kinetics, and characteristics of the Kupffer cells in the normal steady state. *J. Exp. Med.* **1978,** *148* (1), 1-17.
5. Van Furth, R.; Diesselhoff-den Dulk, M., Dual origin of mouse spleen macrophages. *J. Exp. Med.* **1984,** *160* (5), 1273-1283.
6. Liu, F.; Dai, S.; Feng, D.; Qin, Z.; Peng, X.; Sakamuri, S. S.; Ren, M.; Huang, L.; Cheng, M.; Mohammad, K. E., Distinct fate, dynamics and niches of renal macrophages of bone marrow or embryonic origins. *Nat. Commun.* **2020,** *11* (1), 1-16.
7. Penke, L. R.; Speth, J. M.; Draijer, C.; Zaslona, Z.; Chen, J.; Mancuso, P.; Freeman, C. M.; Curtis, J. L.; Goldstein, D. R.; Peters-Golden, M., PGE2 accounts for bidirectional changes in alveolar macrophage self-renewal with aging and smoking. *Life. Sci. Alliance* **2020,** *3* (11).
8. Jiao, Y.; Zhang, J.; Yan, J.; Stuart, J.; Gibson, G.; Lu, L.; Willaims, R.; Wang, Y. J.; Gu, W., Differential gene expression between wild-type and Gulo-deficient mice supplied with vitamin C. *Genet. Mol. Biol.* **2011,** *34* (3), 386-395.
9. Forder, J. S., Mallory Wagner, Margot Schaefer, Rachel J Gorky, Jonathon van Golen, Kenneth L Nohe, Anja Dhurjati, Prasad A Physiologically - Based Pharmacokinetic Model for Targeting Calcitriol - Conjugated Quantum Dots to Inflammatory Breast Cancer Cells. *Clin. Transl. Sci.* **2019,** *12* (6), 617-624.
10. Hall, C.; Lueshen, E.; Linninger, A. A., Interspecies scaling in pharmacokinetics: A novel whole-body physiologically based modeling framework to discover drug biodistribution mechanisms in vivo. *J. Pharm. Sci.* **2012,** *101* (3), 1221-1241.
11. Gjedde, S. B.; Gjeode, A., Organ blood flow rates and cardiac output of the balb/c mouse. *Comparative Biochemistry Physiology--Part A: Physiology* **1980,** *67* (4), 671-674.
12. Davies, B.; Morris, T., Physiological parameters in laboratory animals and humans. *Pharm. Res.* **1993,** *10* (7), 1093-5.

13. Boswell, C. A.; Ferl, G. Z.; Mundo, E. E.; Bumbaca, D.; Schweiger, M. G.; Theil, F. P.; Fielder, P. J.; Khawli, L. A., Effects of anti-VEGF on predicted antibody biodistribution: roles of vascular volume, interstitial volume, and blood flow. *PloS one* **2011,** *6* (3), e17874.
14. Kim, S.-G.; Ackerman, J. J., Quantitative determination of tumor blood flow and perfusion via deuterium nuclear magnetic resonance spectroscopy in mice. *Cancer Res.* **1988,** *48* (12), 3449-3453.
15. Song, C. W.; Kang, M. S.; Rhee, J. G.; Levitt, S. H., The effect of hyperthermia on vascular function, pH, and cell survival. *Radiology* **1980,** *137* (3), 795-803.
16. Mukaka, M. M., A guide to appropriate use of correlation coefficient in medical research. *Malawi. Med. J.* **2012,** *24* (3), 69-71.
17. Nah, B. S.; Choi, I.-B.; Oh, W. Y.; Osborn, J. L.; Song, C. W., Vascular thermal adaptation in tumors and normal tissue in rats. *Int. J. Radiat. Oncol., Biol., Phys.* **1996,** *35* (1), 95-101.
18. Rappaport, D. S.; Song, C. W., Blood flow and intravascular volume of mammary adenocarcinoma 13726A and normal tissues of rat during and following hyperthermia. *Int. J. Radiat. Oncol., Biol., Phys.* **1983,** *9* (4), 539-547.
19. Shakil, A.; Osborn, J. L.; Song, C. W., Changes in oxygenation status and blood flow in a rat tumor model by mild temperature hyperthermia. *Int. J. Radiat. Oncol., Biol., Phys.* **1999,** *43* (4), 859-65.
20. Stapleton, S.; Dunne, M.; Milosevic, M.; Tran, C. W.; Gold, M. J.; Vedadi, A.; McKee, T. D.; Ohashi, P. S.; Allen, C.; Jaffray, D. A., Radiation and Heat Improve the Delivery and Efficacy of Nanotherapeutics by Modulating Intratumoral Fluid Dynamics. *ACS Nano* **2018,** *12* (8), 7583-7600.
21. Kinuya, S.; Yokoyama, K.; Hiramatsu, T.; Tega, H.; Tanaka, K.; Konishi, S.; Shuke, N.; Aburano, T.; Watanabe, N.; Takayama, T.; Michigishi, T.; Tonami, N., Combination radioimmunotherapy with local hyperthermia: increased delivery of radioimmunoconjugate by vascular effect and its retention by increased antigen expression in colon cancer xenografts. *Cancer Lett.* **1999,** *140* (1), 209-218.
22. Kinuya, S.; Yokoyama, K.; Hiramatsu, T.; Konishi, S.; Watanabe, N.; Shuke, N.; Aburano, T.; Bunko, H.; Michigishi, T.; Tonami, N., Optimal Timing of Administration of Hyperthermia in Combined Radioimmunotherapy. *Cancer Biother.Radiopharm.* **2000,** *15* (4), 373-379.
23. Shrivastav, S.; Kaelin, W. G., Jr.; Joines, W. T.; Jirtle, R. L., Microwave hyperthermia and its effect on tumor blood flow in rats. *Cancer Res.* **1983,** *43* (10), 4665-9.
24. Cope, D. A.; Dewhirst, M. W.; Friedman, H. S.; Bigner, D. D.; Zalutsky, M. R., Enhanced delivery of a monoclonal antibody F(ab')2 fragment to subcutaneous human glioma xenografts using local hyperthermia. *Cancer Res.* **1990,** *50* (6), 1803-9.
25. Hauck, M. L.; Dewhirst, M. W.; Bigner, D. D.; Zalutsky, M. R., Local hyperthermia improves uptake of a chimeric monoclonal antibody in a subcutaneous xenograft model. *Clin. Cancer Res.* **1997,** *3* (1), 63-70.

26. Schuster, J. M.; Zalutsky, M. R.; Noska, M. A.; Dodge, R.; Friedman, H. S.; Bigner, D. D.; Dewhirst, M. W., Hyperthermic modulation of radiolabelled antibody uptake in a human glioma xenograft and normal tissues. *Int. J. Hyperthermia* **1995,** *11* (1), 59-72.
27. Song, C. W., Effect of hyperthermia on vascular functions of normal tissues and experimental tumors; brief communication. *Journal of the National Cancer Institute* **1978,** *60* (3), 711-3.
28. Xu, Y.; Choi, J.; Hylander, B.; Sen, A.; Evans, S. S.; Kraybill, W. G.; Repasky, E. A., Fever-range whole body hyperthermia increases the number of perfused tumor blood vessels and therapeutic efficacy of liposomally encapsulated doxorubicin. *Int. J. Hyperthermia* **2007,** *23* (6), 513-527.
29. Winslow, T. B.; Eranki, A.; Ullas, S.; Singh, A. K.; Repasky, E. A.; Sen, A., A pilot study of the effects of mild systemic heating on human head and neck tumour xenografts: Analysis of tumour perfusion, interstitial fluid pressure, hypoxia and efficacy of radiation therapy. *International journal of hyperthermia : the official journal of European Society for Hyperthermic Oncology, North American Hyperthermia Group* **2015,** *31* (6), 693-701.
30. Sen, A.; Capitano, M. L.; Spernyak, J. A.; Schueckler, J. T.; Thomas, S.; Singh, A. K.; Evans, S. S.; Hylander, B. L.; Repasky, E. A., Mild elevation of body temperature reduces tumor interstitial fluid pressure and hypoxia and enhances efficacy of radiotherapy in murine tumor models. *Cancer Res.* **2011,** *71* (11), 3872-80.
31. Stylianopoulos, T.; Martin, J. D.; Chauhan, V. P.; Jain, S. R.; Diop-Frimpong, B.; Bardeesy, N.; Smith, B. L.; Ferrone, C. R.; Hornicek, F. J.; Boucher, Y.; Munn, L. L.; Jain, R. K., Causes, consequences, and remedies for growth-induced solid stress in murine and human tumors. *Proc. Natl. Acad. Sci. USA* **2012,** *109* (38), 15101-8.
32. Olive, K. P.; Jacobetz, M. A.; Davidson, C. J.; Gopinathan, A.; McIntyre, D.; Honess, D.; Madhu, B.; Goldgraben, M. A.; Caldwell, M. E.; Allard, D.; Frese, K. K.; Denicola, G.; Feig, C.; Combs, C.; Winter, S. P.; Ireland-Zecchini, H.; Reichelt, S.; Howat, W. J.; Chang, A.; Dhara, M.; Wang, L.; Rückert, F.; Grützmann, R.; Pilarsky, C.; Izeradjene, K.; Hingorani, S. R.; Huang, P.; Davies, S. E.; Plunkett, W.; Egorin, M.; Hruban, R. H.; Whitebread, N.; McGovern, K.; Adams, J.; Iacobuzio-Donahue, C.; Griffiths, J.; Tuveson, D. A., Inhibition of Hedgehog signaling enhances delivery of chemotherapy in a mouse model of pancreatic cancer. *Science* **2009,** *324* (5933), 1457-61.
33. Jacobetz, M. A.; Chan, D. S.; Neesse, A.; Bapiro, T. E.; Cook, N.; Frese, K. K.; Feig, C.; Nakagawa, T.; Caldwell, M. E.; Zecchini, H. I.; Lolkema, M. P.; Jiang, P.; Kultti, A.; Thompson, C. B.; Maneval, D. C.; Jodrell, D. I.; Frost, G. I.; Shepard, H. M.; Skepper, J. N.; Tuveson, D. A., Hyaluronan impairs vascular function and drug delivery in a mouse model of pancreatic cancer. *Gut* **2013,** *62* (1), 112-20.

34. Provenzano, P. P.; Cuevas, C.; Chang, A. E.; Goel, V. K.; Von Hoff, D. D.; Hingorani, S. R., Enzymatic targeting of the stroma ablates physical barriers to treatment of pancreatic ductal adenocarcinoma. *Cancer Cell*. **2012,** *21* (3), 418-29.
35. Liu, J.; Liao, S.; Diop-Frimpong, B.; Chen, W.; Goel, S.; Naxerova, K.; Ancukiewicz, M.; Boucher, Y.; Jain, R. K.; Xu, L., TGF-β blockade improves the distribution and efficacy of therapeutics in breast carcinoma by normalizing the tumor stroma. *Proc. Natl. Acad. Sci. USA* **2012,** *109* (41), 16618-23.
36. Chauhan, V. P.; Martin, J. D.; Liu, H.; Lacorre, D. A.; Jain, S. R.; Kozin, S. V.; Stylianopoulos, T.; Mousa, A. S.; Han, X.; Adstamongkonkul, P.; Popović, Z.; Huang, P.; Bawendi, M. G.; Boucher, Y.; Jain, R. K., Angiotensin inhibition enhances drug delivery and potentiates chemotherapy by decompressing tumour blood vessels. *Nat. Commun*. **2013,** *4*, 2516.
37. Zhang, B.; Wang, H.; Jin, K.; Jiang, T.; Shen, S.; Luo, Z.; Tuo, Y.; Jiang, X.; Liu, X.; Hu, Y.; Pang, Z., BQ123 selectively improved tumor perfusion and enhanced nanomedicine delivery for glioblastomas treatment. *Pharmacol. Res*. **2018,** *132*, 211-219.
38. Wei, Y.; Song, S.; Duan, N.; Wang, F.; Wang, Y.; Yang, Y.; Peng, C.; Li, J.; Nie, D.; Zhang, X.; Guo, S.; Zhu, C.; Yu, M.; Gan, Y., MT1-MMP-Activated Liposomes to Improve Tumor Blood Perfusion and Drug Delivery for Enhanced Pancreatic Cancer Therapy. *Adv. Sci*. **2020,** *7* (17), 1902746.
39. Sorace, A. G.; Quarles, C. C.; Whisenant, J. G.; Hanker, A. B.; McIntyre, J. O.; Sanchez, V. M.; Yankeelov, T. E., Trastuzumab improves tumor perfusion and vascular delivery of cytotoxic therapy in a murine model of HER2+ breast cancer: preliminary results. *Breast. Cancer. Res. Treat*. **2016,** *155* (2), 273-84.
40. Yeow, Y. L.; Kotamraju, V. R.; Wang, X.; Chopra, M.; Azme, N.; Wu, J.; Schoep, T. D.; Delaney, D. S.; Feindel, K.; Li, J.; Kennedy, K. M.; Allen, W. M.; Kennedy, B. F.; Larma, I.; Sampson, D. D.; Mahakian, L. M.; Fite, B. Z.; Zhang, H.; Friman, T.; Mann, A. P.; Aziz, F. A.; Kumarasinghe, M. P.; Johansson, M.; Ee, H. C.; Yeoh, G.; Mou, L.; Ferrara, K. W.; Billiran, H.; Ganss, R.; Ruoslahti, E.; Hamzah, J., Immune-mediated ECM depletion improves tumour perfusion and payload delivery. *EMBO Mol. Med*. **2019,** *11* (12), e10923.
41. Zheng, X.; Fang, Z.; Liu, X.; Deng, S.; Zhou, P.; Wang, X.; Zhang, C.; Yin, R.; Hu, H.; Chen, X.; Han, Y.; Zhao, Y.; Lin, S. H.; Qin, S.; Wang, X.; Kim, B. Y.; Zhou, P.; Jiang, W.; Wu, Q.; Huang, Y., Increased vessel perfusion predicts the efficacy of immune checkpoint blockade. *J. Clin. Invest*. **2018,** *128* (5), 2104-2115.
42. Shen, Y.; Li, S.; Wang, X.; Wang, M.; Tian, Q.; Yang, J.; Wang, J.; Wang, B.; Liu, P.; Yang, J., Tumor vasculature remolding by thalidomide increases delivery and efficacy of cisplatin. *J. Exp. Clin. Cancer. Res*. **2019,** *38* (1), 427.